Muscle Activation Profile While Walking with Perturbations

Uri Rosenblum[1,2], Itshak Melzer[2], Gabi Zeilig[3,4], Meir Plotnik*[1,5,6]

[1] Center of Advanced Technologies in Rehabilitation, Sheba Medical Center, Tel Ha'shomer, Israel.

[2] Department of Physical Therapy, Recanati School for Community Health Professions, Faculty of Health Sciences, Ben-Gurion University of the Negev, Be'er Sheva, Israel

[3] Department of Neurological Rehabilitation, Sheba Medical Center, Tel HaShomer, Israel

[4] Department of Physical and Rehabilitation Medicine, Sackler Faculty of Medicine, Tel Aviv University, Israel

[5] Department of Physiology and Pharmacology, Sackler Faculty of Medicine, Tel-Aviv University, Tel Aviv, Israel

[6] Sagol School of Neuroscience, Tel Aviv University, Tel Aviv, Israel

Running head: MUSCLE SPECTRAL PROFILE WHILE WALKING WITH PERTURBATIONS

Corresponding Author: Meir Plotnik, Ph.D., Rehabilitaion Hospital, Chaim Sheba Medical

Center, Tel Hashomer, 5265601, Israel

Fax: +972-3-5303821

Tel: +972-3-5307508

e-mail: meir.plontik@sheba.health.gov.il

Abstract

To avoid falling consequential to unexpected balance loss i.e., perturbation, requires people to readjust their footing rapidly and effectively (i.e., recovery stepping response). We aimed to investigate lower limb muscle activation and differences between ankle and knee muscle recruitment due to unexpected support-surface perturbations during walking. This was measured by frequency content changes of surface electromyography (sEMG). Twenty adults (27.00±2.79 years, 10 females) were exposed to perturbations while walking on a treadmill in virtual reality environment. Perturbations were applied randomly in different phases of gait in 4 directions (i.e., anterior/posterior/right/left). sEMG signals from the tibialis anterior (TA) and vastus lateralis (VL) muscles were studied. sEMG total spectral power for all signal frequencies and for specific bands (40-150 Hz, 150-250 Hz, 250-400 Hz) were compared 4 seconds before perturbation (i.e., baseline) versus four seconds after perturbations. We found that compared to baseline there was a significant increase in the total spectral power of lower-extremity muscles at the first 3 seconds after perturbation, for all frequencies. TA had a significant differential change in frequency bands: 150-250Hz>40-150Hz, while VL demonstrated a different differential response in frequency bands 40-150Hz & 150-250Hz>250-400Hz. Both muscles showed an increase in total spectral power for the first second after perturbation followed by gradual decrease to baseline total spectral power subsiding after 3 seconds. Our findings suggest that muscle operating frequency is modulated in real time to fit functional goal requirements such as a rapid change of footing in response to unexpected loss of balance.

Key words: walking perturbations; spectral power; muscle fibers; muscle function; balance recovery

New & Noteworthy: To study muscle spectral profiles in response to loss of balance, we investigated the dynamics of muscle spectral power changes, across different frequency bands after unannounced physical perturbations during walking. Our analysis showed increased activation of high-frequency motor units of the lower-limb muscles, subsiding 3 seconds after perturbation. Differential power increase of specific frequency bands suggests that muscle activation is modulated in real time to fit functional goal requirements.

Introduction

Stability while walking is maintained by utilizing two mechanisms. The first is *postural orientation*: active body alignment with respect to gravity, the supporting surface, and visual environment. Postural orientation is achieved through integration of somatosensory, visual and vestibular information. Sensory information is reweighted constantly by the central nervous system (CNS) to maintain postural orientation by engaging anti-gravity muscles of the lower-limbs, trunk and even upper-limbs muscles. The second mechanism is termed *postural equilibrium*: active control over the placement of the body center of mass (CoM) commensurate with its velocity and within boundaries of its base of support (BoS) provided by the feet (17, 21). Thus, in response to external- or self-disturbances to stability, the CNS utilizes these mechanisms, by means of coordinating movement between arms, trunk and lower-limb muscles, to maintain equilibrium (2, 21, 41).

In laboratory settings, unexpected external perturbations are introduced in different phases of the gait cycle to provoke postural disturbances. To avoid falling, individuals make rapid, reflex-like reactive balance responses to modulate their BoS (i.e., footing) by stepping in the direction of the CoM velocity (4, 20). This reactive balance

response (i.e., compensatory stepping response) was reported to be under spinal, supraspinal and cortical control (4, 24). It is characterized by sequences of movement strategies (e.g., outward & inward stepping) and muscle activity can be measured using surface electromyography (sEMG) to describe muscle recruitment patterns and synergies (2, 6, 18–20, 41).

In the last two decades studies have started to investigate the effect of concurrent cognitive task (i.e., a cognitive dual task) on balance reactive performance to perturbations while standing and walking (43). These studies suggest that balance control during standing and walking requires cognitive resources. Effectively the dual task delayed reaction times to perturbations, as was measured by sEMG, and changed the activity in motor and sensory brain regions (3, 28, 30, 31, 33, 36). Hof et al. (20) demonstrated that in response to medio-lateral perturbations, when the CoM is pushed inward in relation to the stepping limb, an outward stepping strategy is performed. Likewise, when the CoM is pushed outward in relation to the stepping limb, an inward stepping strategy is performed. At the extreme of the inward stepping strategy is the cross-over stepping strategy (see Fig. S1 at https://doi.org/10.6084/m9.figshare.13562789.v1). These reactions (i.e., changes to the regular footing) are scaled in relation to CoM displacement and velocity magnitudes.

sEMG measurements literature shows that compensatory stepping responses are accompanied by elevated sEMG activity of the distal (32, 41) and proximal (41) lower limb muscles (e.g., see Fig. 1). Additional studies show increased ankle muscle activation (i.e., tibialis anterior, soleus, peroneus longus) of the limb in stance (6, 19). The CNS has two general means to control the force exerted by skeletal muscles: alter the number of active motor units, called recruitment; and modulate the rate of action-potential impulses (i.e., frequency) driving motor units, called rate coding. Motor units

are recruited by size (i.e., *the size principle*) from those that produce the smallest forces to those that exert the largest forces (11, 15, 34, 46). Both animal and human studies indicate that frequency content of muscle sEMG signals are related to muscle fiber type and cross-sectional area ratio (i.e., the ratio between different muscle fiber types in each cross-sectional area of the muscle) (27, 42). In humans, lower frequencies, i.e, 40-60 Hz are attributed to the activity of small alpha-motoneurons and related type I fibers, 60-120 Hz frequencies are attributed to medium alpha-motoneurons and related type IIa fibers (oxidative fibers) and the higher frequencies,170-220 Hz, are attributed to the large alpha-motoneurons and their related type IIb fibers (glycolytic fibers) (42). sEMG spectral density is analogous to a non-invasive "electrical biopsy". It can be used to estimate fiber type cross-sectional area in muscles, or to identify pathological and age-related changes in fiber-type cross-sectional area (7). Two main sEMG signals' properties, that affect the frequency spectrum, are the firing behavior of the motor units (i.e., synchronization and clustering), and the shape of the motor unit action potential (1, 10, 44). In recent years, there has been growing interest in muscle activation frequency while walking (5, 23, 38, 47). To the best of our knowledge, no research to date has examined muscle spectral power density in response to unexpected loss of balance during walking, and subsequent balance recovery steps.

Here we aimed to investigate the progression of lower limb activation pattern after unannounced perturbations while walking as measured by sEMG. We examined whether sEMG frequencies change in response to unannounced loss of balance (i.e., perturbations) and how muscle signature frequencies change over time in both ankle and knee muscles. Three hypotheses drive the present work: (1) Total spectral power for all frequencies would increase due to unannounced support-surface perturbations, then gradually decrease; (2) Total spectral power of higher sEMG frequencies will

increase more rapidly than the increase seen in the lower frequencies, due to the rapid footing correction to maintain balance (i.e., rapid force exertion) (9, 40) ; (3) As TA muscles are strongly implicated in balance recovery while walking (20), and perform finer movements than VL (i.e., shifting the pressure under the foot to contain the body CoM) we hypothesized that the TA muscle will demonstrate greater change in high frequency bands compared to the VL muscle, similar to the results found by Seki and Narusawa (40) for hand muscles.

Methods

Participants

Twenty healthy adults participated in this study (Table 1). Exclusion criteria were: obesity (i.e., body mass index [kg/m^2] > 30) (25); orthopedic conditions affecting gait and balance (e.g., total knee replacement, total hip replacement, ankle sprain, limb fracture); cognitive loss or psychiatric conditions; cardiac conditions (e.g., non-stable ischemic heart disease, congestive heart failure); chronic obstructive pulmonary disease; and neurological diseases associated with loss of balance (e.g., multiple sclerosis, myelopathy). The study protocol was approved by the Institutional Review Board of Sheba Medical Center). All participants provided written informed consent prior to entering the study. Part of the cohort was used for a different data set (39).

Table 1: Demographic and physical characteristics (Mean ±SD)

	Participants (N = 20)
Age (years)	27.00 ±2.79
Sex (F/M)	10/10
Height (m)	1.67 ±0.08

Weight (Kg)	62.54 ±10.65
BMI (kg/m^2)	22.22 ±2.63
Years of education	15.35 ±2.16

Abbreviations: SD=Standard Deviation; BMI=Body Mass Index

Apparatus and settings

Set-up for the experiment is described elsewhere in detail (39). Briefly, participants walked in the CAREN High-End (Motek Medical B.V., Amsterdam, Netherlands) virtual reality system, equipped with a split-belt treadmill mounted on a platform that can be moved in six degrees of freedom. The platform is positioned in the center of a 360° dome-shaped screen.

Unannounced support-surface perturbations along the anterior-posterior plane occurred by reducing the speed of one belt (split-belt treadmill) by 1.2 m/s with a deceleration of 5 m/s^2. Right-left unannounced support-surface perturbations occurred by shifting the platform 15cm for 0.92 seconds, either left or right. Eighteen Vicon (Vicon Motion Systems, Oxford, UK) motion capture cameras placed around the dome's circumference along with force plates under the treadmill's belts, allowed for continuous recording of kinetic (ground reaction forces) and kinematic (motion) data for real-time/post-hoc gait phase detection. Perturbation control and data recording were done by two computers that integrated kinetic, kinematic and perturbation data.

sEMG recording

sEMG data were collected from vastus lateralis (VL) and tibialis anterior (TA) muscles, known to take part in postural orientation and equilibrium (5, 19, 32, 35, 41).

sEMG signals were recorded using bipolar hydrogel surface electrodes, 10mm in diameter, 24mm apart, placed parallel to muscle fibers, consistent with SENIAM guidelines (16). The ground electrode was placed on spinous process of C7. Before electrode application, participants' skin was shaved and cleaned with an abrasive pad and alcohol to reduce skin impedance. Finally, electrodes and cables were secured to the skin with tape to reduce moving artifacts.

sEMG signals were tested for specific movements to control for crosstalk effects. Raw sEMG signals were recorded on a tablet computer (Lenovo ThinkPad) at 2048 Hz using an Eego referential amplifier (eemagine Medical Imaging Solutions GmbH, Berlin, Germany), with an input impedance (referential) >1GΩ, and weight < 500g.

Protocol

Participants first acclimated to walking in virtual reality (see (39) for more details). They walked at a comfortable, self-selected speed (using the system's self-paced mode (37) while subjected to random, unannounced perturbations at different phases of the gait cycle. Perturbations varied in direction (anterior-posterior/right-left) and gait cycle phase presentation (double support/single support). The experimental set-up minimized anticipation reactions to perturbation. Trials were conducted under two conditions: *single task* (i.e., only walking with perturbations) and *dual task*, during which the participants were asked to perform arithmetic calculations while walking with perturbations. Our experimental design minimized anticipatory responses by randomly varying perturbations across different gait phases to be more ecologically valid. Time intervals between consecutive perturbations also randomly varied to minimize anticipation effect. Experiments consisted of 4 perturbation trials with 2 min recesses between them to minimize fatigue (see Fig. 1 for illustration). Two trials

were performed in single task condition and two in dual task condition (24 perturbations in every condition). The cognitive dual task consisted of a concurrent arithmetic calculation, based on a paced auditory serial addition test (14). Participants could rest at any time (39).

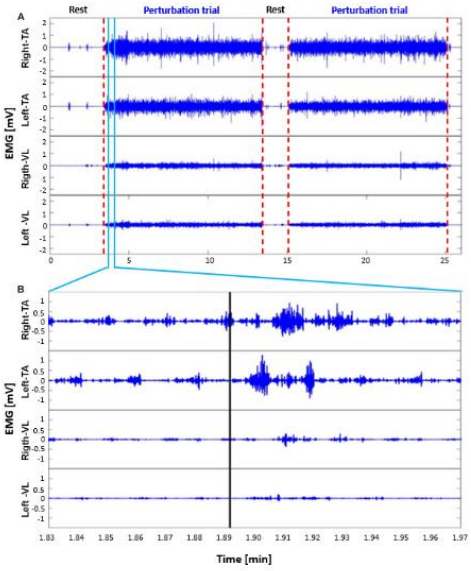

Fig.1: Filtered surface electrophysiological, sEMG. Data for 2 exemplary, consecutive trials (A) and for one specific perturbation in a window of 4 seconds before and after the perturbation (B), of left and right tibialis anterior (TA) and vastus lateralis (VL). From the traces we can see that TA activity is greater than VL activity for the whole 2 trials and in the specific perturbation. Worth noting that the signals in panel A maintain relatively constant amplitude throughout the trials, indicating no effects of fatigue. Additionally, in panel B we can see the muscle response very evident in the first 2 seconds after perturbation onset (black vertical line) after which it gradually returns to pre-perturbation values.

sEMG data handling, processing, and analyses

sEMG data were preprocessed and analyzed across frequency domains using customized scripts written in MATLAB version R2019b (Mathworks, Nathick USA). Raw sEMG signals were first band-pass filtered (40–1000 Hz) (35) with a 500th order Butterworth filter. Filtered sEMG signals were sliced in 1-minute windows around perturbation events (i.e., 30 sec. prior to 30 sec. after) and grouped as baseline data, average of four seconds of undisturbed walking segment prior to the perturbation, and 4 seconds of balance and walking recovery after perturbation (Time1-4, respectively). These segments were selected consistent with existing research from our group, examining recovery of step length and width in response to unexpected walking perturbations (39). Perturbations were classified according to the compensatory

stepping responses they elicit (i.e., inward or outward first step after perturbation) and analyzed separately, both left and right.

sEMG data processing consisted of two main steps following the procedures described by Garcia-Retortillo et al. (12). In the first step, we quantified total spectral power, S(f), for averaged activity at baseline and Time1-4, for each muscle (i.e., right and left TA, and VL,), by calculating the area under curves in Fig.2. We used the 'pwelch' built-in MATLAB function to extract spectral power for each muscle and for every walking segment (i.e., baseline & Time1-4), using a time window of 100ms, with an overlap of 50ms. For each time window, we calculated total spectral power (S(f)) across all frequencies (12):

(Eq.1)

$$S(f) = \sum_{i=1}^{N} S(fi)$$

Where *fi* are all frequencies in the analysis, and N is the number of discrete frequency values for each segment.

To quantify differences in spectral power between segments, we calculated median total spectral power for each muscle, by calculating the area under the curves of Fig. 2. In the second step, we measured the sequence in total spectral power over time from baseline to Time4 for each segment (see Figs. 2 and 3). We then examined the frequency spectrum of each segment in the following bands: 40-150Hz, 150-250Hz, 250-400Hz, 400-800Hz, and 800-1000Hz, based on (12) and our data, presented in Fig. 2 and the progression of each frequency band in time (from baseline to Time4). Average spectral power (due to the different frequency band width) for every frequency band, in every segment was calculated using the following (12):

(Eq.2)

$$< S(f) >= \sum_{i=1}^{M} S(fi)/M$$

Where f_i are all frequencies in every frequency band, and M is the number of spectral power values in that frequency band. To specifically measure rate and magnitude of change across different frequency bands over time, we calculated change from baseline, for every frequency band, in every segment where, *fb* is the frequency band in every segment *x* (Time1-4) and *bl* is for the baseline segment:

(Eq.3)

$$\Delta\, ratio\ = (S(fb)x - S(fb)bl)/S(fb)bl$$

For this study, we examined results for the left TA (ankle stabilizing muscle of the non-dominant limb) and the left VL (anti-gravity muscle of the non-dominant limb), in response to right platform translation during stance of the left leg i.e., before right foot initial contact. Results are similar for all muscles across different perturbation types. Research examining muscle synergy activated in response to perturbations while walking in self-paced mode show the TA and VL participate in all synergies. (6).

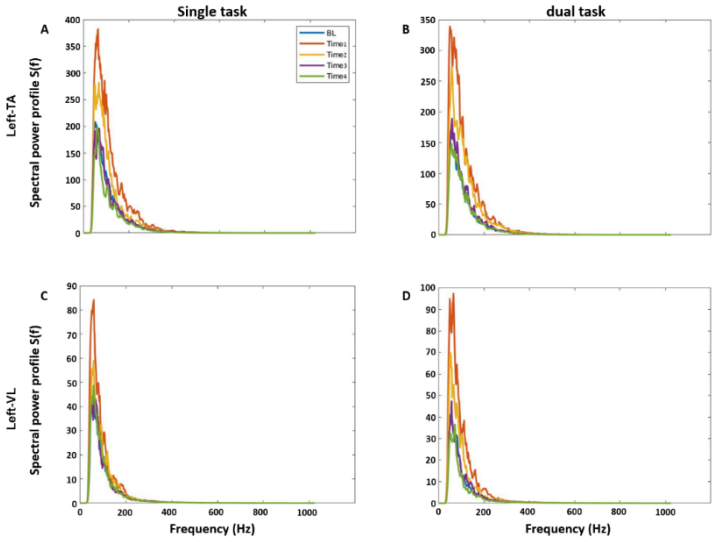

Fig. 2: Progression of total spectral power (mV^2/Hz) over time in response to unexpected perturbations eliciting an inward stepping response with the right leg. Ankle left tibialis anterior (TA) muscle and knee, left vastus lateralis (VL) muscle (A, B and C, D, respectively) are depicted under concurrent cognitive task (dual task) and without (single task). Traces represent grand averages across all participants (n=20). For both muscles the total spectral power peaks in the 1st second after perturbation (Time1, red trace), decrease dramatically in Time2 (yellow trace) and then

gradually returns to baseline (baseline) levels after ~3 seconds (magenta trace). Please note that the Time3 and Time4 traces almost completely overlap with the baseline trace, indicating return to baseline. Surface electromyographic (sEMG) spectral power profiles are similar in shape but differ in magnitude between ankle and knee muscles, in baseline as well as in the four seconds after perturbation (Time1-4, see key); The spectral power of left TA is higher than left VL throughout, indicating a relationship between muscle function and spectral power.

Statistical analyses

To test our first hypothesis (between-segment spectral power comparisons, across frequencies), we computed mixed-effect models with repeated measures to account for dependence of observations within participants. Since data did not distribute normally values were Ln transformed to fit a normal distribution. The transformed change was used as independent variables while time segments, muscles and condition (i.e., single/dual task) along with the interactions of muscles X time segment, time segments X condition, and muscles X condition and time segment X muscles X condition functioned as within-subject variables. Least significant difference was applied to account for multiple post-hoc comparisons. To test our second and third hypotheses (differences in change in frequency bands across segments over time, TA muscle will demonstrate greater change in high frequency bands compared to the VL muscle) and to analyze total spectral power progression across frequency bands, we computed mixed-effect models with repeated measures to account for dependence of observations within participants. In each frequency band, we calculated change in total spectral power over time. Since data did not distribute normally and it had negative values, they were shifted by 2 and Ln transformed to fit a Gamma distribution. The transformed change was used as independent variables while time segments, frequency bands, muscles and condition along with the interactions of muscles X frequency band, time segments X condition, and muscles X time segments X frequency band functioned as within-subject variables in mixed-

effect models. Least significant difference was applied to account for multiple post-hoc comparisons. Statistical significance was set *a priori* at $p<0.05$. Data were analyzed using MATLAB version R2019b and SPSS version 23 (IBM Inc., Chicago, IL).

Results

Spectral power distribution at baseline and four seconds after perturbation for all frequencies

Spectral power distribution for the left TA and VL before and after perturbations are presented in Fig. 2. S(f) (i.e., area under curve of profiles in Fig.2) is presented in Fig.3. The mixed-effect model showed significant main effect for time segment ($F_{[4,2180]}$ = 57.98, $p<0.001$) and muscle ($F_{[1,2180]}$ = 1275.20, $p<0.001$) and no significant main affect for condition ($F_{[1,2180]}$ = 2.30, $p=0.13$). More specifically, there was a significant increase in muscle activation for all frequencies in Time1 & Time2, as compared to baseline ($p<0.001$). S(f) increased rapidly in Time1 and then gradually and significantly diminishes during every consecutive second (not including Time4) for both left TA and VL muscles ($p<0.001$), see Fig.3 and Table 2. We found significantly higher S(f) for left TA muscle than left VL muscle in all time segments (i.e., baseline-Time4, $p<0.001$). Although no main effect was found for condition we did find an interaction effect between condition and muscle ($F_{[1,2180]}$ = 5.30, $p=0.02$). Post-hoc analysis showed that the left VL muscle drives the interaction ($F_{[1,2180]}$ = 7.29, $p=0.007$) with higher S(f) for dual task condition compared to single task condition ($p=0.007$).

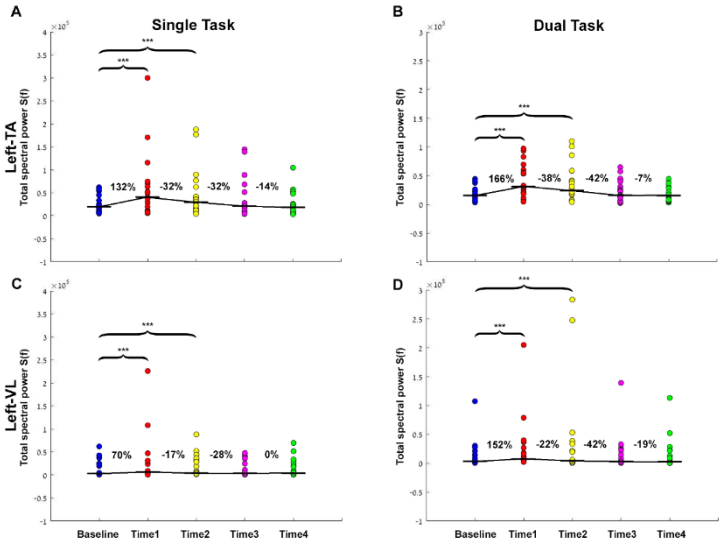

Fig3: Group medians (black horizontal lines) for every time segment, and mean value for every participant (circles in every time segment, n=20) at baseline (4 seconds prior to perturbation) and for the 4 seconds after perturbation in bins of one second (Time1-4), for all frequencies. Values were calculated from the area under the spectral power profiles in Fig. 2 (Colors are consistent with Fig. 2.). (A) left tibialis anterior (TA) muscle in single task condition; (B) left TA in dual task condition; (C) left vastus lateralis (VL) muscle in single task condition; (D) left VL muscle in dual task condition. Panel (A): TA increase total power by 132% in Time1, then decrease total power in 32% in Time2 and Time3, and 14% in Time4. Panel (B): TA increase total power by 166% in Time1, then decrease total power in 38% in Time2, 42% in Time3, and 7% in Time4. Panel (C): left VL increase total spectral power by 70% in Time1, then decrease total spectral power by 17% in Time2, 28% in Time3, and 0% in Time4. Panel (D): left VL increase total spectral power by 152% in Time1, then decrease total spectral power by 22% in Time2, 42% in Time3, and 19% in Time4. See text for interpretation of findings. The percentages indicate the relative change from second to second for the entire cohort (n=20).

*** p<0.001

Table2: total spectral power ($\mu V^2/Hz$) for left tibialis anterior (TA) and left vastus lateralis (VL) over time[a,b,c]

	Baseline	Time1	Time2	Time3	Time4
TA	22414±17482[d]	69526±46020[d,e,f,g,h]	42352±53646[d,e,g,h]	30918±71305[d]	21170±17606[d]
	(2291-125977)	(2232-920650)	(1579-581471)	(1226-1014129)	(929-104664)
VL	7690±18213	25188±79512[e,f,g,h]	17307±55667[e,g,h]	8941±23348	8122±19952
	(375-162224)	(349-950522)	(168-617012)	(130-201554)	(114-161384)

a, Values are Mean ±SD (Range).
b, n=220 for every time segment.
c, Within each muscle, Time1 & Time2 > baseline and Time1>Time2>Time3 significantly.
The least significant difference adjusted significance level is 0.05 (see text for full report on statistical results).
d, significantly larger than left VL.

e, significantly larger than corresponding value for baseline.
f, significantly larger than corresponding value for Time2.
g, significantly larger than corresponding value for Time3.
h, significantly larger than corresponding value for Time4.

Leg muscles frequency band Change relative to baseline in response to unexpected perturbations and progression over time

Because frequencies greater than 400 Hz contributed less than 1% to total spectral power of all frequencies, the analyses were restricted to frequencies less than 400 Hz (see Fig. S2 at https://doi.org/10.6084/m9.figshare.13562807.v1). The mixed-effect model ($F_{[47,5232]} = 21.72$, $p<0.001$) shows a significant main effects for time ($F_{[3,5232]} = 298.53$, $p<0.001$). Significant change in total spectral power from baseline from largest to smallest was Time1>Time2>Time3, ($p<0.014$; see Table 3), showing the result in the first model is robust. We also found a significant main effect for frequency band ($F_{[2,5232]}= 14.69$, $p<0.001$). Changes in 40-150 Hz & 150-250 Hz > 250-400 Hz bands ($p<0.028$). Finally, we found a main effect for condition ($F_{[1,5232]}= 24.42$, $p<0.001$). Specifically, under dual task condition there was a greater change in S(f) from baseline compared to single task.

A significant interaction was found between muscle and frequency band ($F_{[2,5232]}= 12.76$, $p<0.001$, see results in table 4). Also significant interaction between time segment and condition was found ($F_{[3,5232]} = 6.86$, $p<0.001$, see results in table 5). Finally, a significant interaction effect between time, frequency band and muscle was found ($F_{[6,5232]} = 2.15$, $p=0.045$, Fig. 4). Post-hoc analyses revealed significantly greater change in 150-250 Hz band than 40-150 Hz band immediately post perturbation, at Time1, for TA ($p=0.047$). The change for 150-250Hz was significantly greater for TA than VL in Time1 ($p=0.046$). For VL we found significantly greater change in 40-150 Hz & 150-250 Hz bands than 250-400 Hz band immediately post perturbation, at Time1 ($p<0.032$), and 40-150 Hz > 250-400 Hz band in Time2 ($p=0.029$). The change for 40-

150 Hz was significantly greater for VL than TA in Time1 (p=0.035). We did not find a significant interaction effect for condition and muscle and time segment and band (p=0.99).

Table 3: Change in total spectral power for left tibialis anterior (TA) and left vastus lateralis (VL) over time[a,b,c].

	Time1	Time2	Time3	Time4
TA	3.34±7.47	1.18±2.25	0.40±1.39	0.29±1.48
	(-0.88-100.59)	(-0.90-22.84)	(-0.97-20.82)	(-0.95-16.91)
VL	4.71±24.19	2.15±12.64	0.37±1.16	0.76±7.89
	(-0.95-451.68)	(-0.96-248.32)	(-0.97-12.73)	(-0.98-164.02)

a, Values are Mean ±SD (Range).
b, n=620 for each muscle at every time segment.
c, Within each muscle, Time1>Time2>Time3 significantly. No differences were found in the change of total spectral power from baseline between the muscles.
The least significant difference adjusted significance level is 0.05 (see text for full report on statistical results).

Table 4: Change in total spectral power for left tibialis anterior (TA) and left vastus lateralis (VL) by frequency band[a,b,c].

	40-150 Hz	150-250 Hz	250-400 Hz
TA	1.08±3.68[d]	1.65±5.64	1.18±3.11
	(-0.94-82.04)	(-0.97-100.59)	(-0.97-29.44)
VL	2.90±18.27[e]	1.91±12.73[e]	1.18±10.86
	(-0.97-451.68)	(-0.98-339.29)	(-0.98-248.32)

a, Values are Mean ±SD (Range)
b, n=880 for each muscle in every frequency band.
c, For left VL, 40-150 Hz & 150-250 Hz > 250-400 Hz band.
d, significantly smaller than left VL.
e, significantly larger than corresponding value for 250-400 Hz band.
The least significant difference adjusted significance level is 0.05 (see text for full report on statistical results).

Table 5: Change in total spectral power for single task (ST) and dual task (DT) conditions over time[a,b,c].

	Time1	Time2	Time3	Time4
ST	2.65±7.59[d,e,f]	1.05±3.80 [e,f]	0.37±1.49	0.32±1.45
	(-0.95-118.47)	(-0.96-85.88)	(-0.97-20.82)	(-0.95-16.91)
DT	5.47±24.40[d,e,f,g]	2.31±12.41[d,e,f,g]	0.40±1.02	0.74±8.00
	(-0.78-451.68)	(-0.90-248.32)	(-0.93-8.99)	(-0.98-164.02)

a, Values are Mean ±SD (Range).
b, n=678 for each muscle at every time segment.
c, Within each muscle, Time1>Time2>Time3 significantly. No differences were found in the change of total spectral power from baseline between the conditions.
d, significantly larger than corresponding value for Time2.
e, significantly larger than corresponding value for Time3.
f, significantly larger than corresponding value for Time4.
g, significantly larger than ST.

The least significant difference adjusted significance level is 0.05.

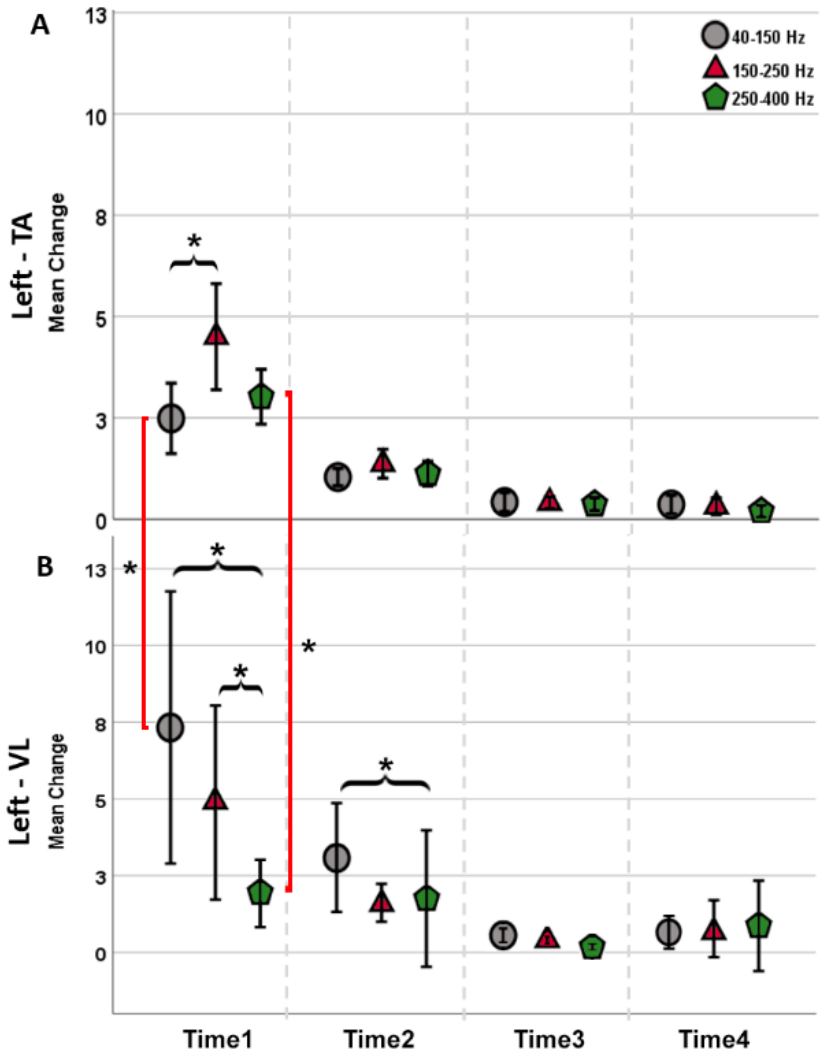

Fig. 4: Mean change (whiskers represent 95%CI of the mean) comparisons for interaction effect between muscle (i.e., left tibialis anterior; TA – panel A, and left vastus lateralis; VL – panel B) time (i.e., 1-4 seconds after perturbation onset; Time1-4) and frequency band (black circle = 40-150 Hz, red triangle = 150-250 Hz, and green pentagons = 250-400 Hz) on change in total spectral power calculated using Eq.3, see *METHODS* (n=5280).

* The least significant difference adjusted significance level < 0.05.

Discussion

The results of the present study support our hypothesis that the total spectral power for all frequencies increased due to loss of balance i.e., unannounced support-surface perturbations, then gradually decrease after 1 second. A significant increase was found in the total spectral power in all frequencies in TA and VL immediately after perturbation followed by gradual decrease (Fig. 3). Our second hypothesis was partially confirmed, the second mixed-effects model showed an increase in total spectral power in the 150-400 Hz frequency bands immediately after perturbation (i.e., Time1) for the ankle, TA muscle and in 40-250 Hz for the VL muscle. We posit that these results are related to engagement of muscle fiber sub-types, fiber sub-types cross sectional area (i.e., muscle architecture), and force control strategies (9, 26, 40, 46) amongst other biological characteristics (13).

Spectral power distribution and change over time for all frequencies

An increase in total spectral power for all frequencies in the first second after unannounced perturbations are in accordance with previous research(6, 20, 42). The increase in total spectral power for all frequencies was followed by a gradual, yet significant, decrease compared to the total spectral power at baseline, ending after 3 seconds. The relatively prolonged elevated spectral power suggests the recovery process, which continues past the initial balance recovery response after perturbation (i.e., first 2-3 steps after perturbation (20, 29, 45)), is accompanied by increased muscle activation. The fact that the recovery process lasts several seconds beyond the initial response is collaborated when observing kinematic outcomes (i.e., step length and width) as was described previously in details (39) .

The role of muscle fibers sub types in Responses to perturbations

Muscle activation spectral power signatures provide information on the muscles' functional roles in locomotion (i.e., baseline walking in our study) and during recovery processes. Our non-invasive "electrical biopsy" (i.e., sEMG) results confirm that there is a modulation of fiber type activation of muscles in response to unannounced perturbations while walking. Type II muscle fibers of the left TA and VL muscles were engaged as part of the rapid balance recovery response. This is expressed by the elevation in the higher frequencies (i.e., 60-400 Hz) in response to the perturbations. However, for TA the response was (Type IIb, glycolytic fibers) oriented (i.e., higher increase in 250-400 Hz) while VL displayed a mixed, Type I and Type II fibers orientation (i.e., higher increase in 40-150 Hz).

Differential effect between muscles

At the physiological level, the engagement of muscle activation for balance recovery was relatively greater for TA than VL (see Table 2 and Fig 3). We postulate that the muscles' size difference along with their required function while walking and in response to perturbation explains this difference. The TA muscle fiber size is much smaller than VL, as a result during dynamic movement such as walking and balance reactions to perturbations the extra load on the joints drives it to exert higher total spectral power. In response to unannounced perturbations, VL must maintain postural orientation, preventing the knee joint from collapsing under the body weight. The ankle muscles are mainly utilized for postural equilibrium, controlling ankle joint movements to redistribute ground pressure under the sole of the foot, effectively shifting the BoS and reducing the magnitude of a balance recovery step (20). The TA specifically assists in stabilizing the ankle by putting it in closed pack position (i.e., The joint position in which articulating bones have their maximum area of contact

with each other), effectively reducing the degrees of freedom the CNS must account for.

The effect of frequency bands on total spectral power change and progression over time

Our results indicate that each frequency band, 40-150 Hz & 150-250 Hz, associated with type I and mixed type I and II muscle fibers, contribute more than 250-400 Hz band (associated with Type II glycolytic muscle fibers) to total spectral power. This result is in accordance with previous literature describing the size principal (11, 35). We found that for frequency band effect on total spectral power change, for all segments, higher frequencies (associated with muscle fibers type IIb) change more than lower frequencies compared to baseline (i.e., 150-250 Hz >40-150 Hz) for the left TA but not the left VL, where 40-150 Hz & 150-250Hz>250-400Hz. The interaction between time frequency band and muscle indicates that this behavior is significant in the first second after perturbation for the left TA. For left VL in the first second after perturbation (Time1), 40-150 Hz & 150-250Hz > 250-400Hz and for Time2, 40-150 Hz>250-400Hz. This suggests that the firing rate of TA, relatively small muscle fibers with fine motor function in balance recovery process, motoneurons increase more than the VL's during balance recovery following unannounced perturbations. Therefore, our results suggest that the rate coding strategy is the main mechanism used to increase muscle force in the TA. The VL exhibits a significant increase at lower (40-150 Hz) and middle (150-250 Hz) frequencies suggesting a mixed mechanism for force control combining rate coding and recruitment strategies. Other studies (e.g., (40)) found similar results for isometric contractions in different muscles with varying force.

When exploring the cross-sectional area of type I and II muscle fibers of the TA and VL, Gregory et al. (13) showed the cross-sectional area of type I muscle fibers were smaller and type II muscle fibers larger than for the VL, resulting in a larger type II: type I-muscle fiber cross-sectional area in the TA. This could provide another explanation of different patterns of frequency activation between TA and VL found in our study. In response to a perturbation requiring a rapid response, the larger type II: type I-muscle fibers cross-sectional area of the TA is expressed in higher frequency compared to VL.

Cognitive load effect on muscle activation in response to unannounced perturbations while walking

Our results indicate that the first 2 seconds after unannounced perturbation are prone to be affected by cognitive dual task, expressed in higher change in total spectral power from baseline in the dual task condition (see Table 5). This result is in agreement with earlier studies that suggested that balance control during standing and walking requires cognitive resources of attention. These showed that performing a concurrent cognitive task while maintaining balance in response to perturbations delayed reaction times to perturbations, as was measured by sEMG, and changed the activity in motor and sensory brain regions (3, 28, 30, 31, 33, 36).

Findings described herein should be considered in the context of several limitations. First, results based on a relatively small number of healthy young adults (n=20). But, since participants were exposed to 46 perturbations on average, the protocol provided hundreds of perturbations, necessary to perform reliable analyses of the total spectral power profiles and its progression over time. Furthermore, sEMG signals are sensitive to movement artifacts caused by: (a) the muscle movement

underneath the skin, and (b) when a force impulse travels through the muscle and skin underlying the sensor causing a movement at the electrode-skin interface (8, 22). These effect mainly the lower frequency domain < 20 Hz (8). The amplifier technical specifications (input impedance >1GΩ) and filtering method of using a bandpass filter of 40-1000 Hz as recommended for walking (35) are sufficient to remove movement artifacts leaving a 'clean' sEMG signal in our range of interest. Finally, since only young adults were examined the results may not be generalizable to middle-aged or older populations. Thus, future study should be conducted to characterize the time-frequency domain of sEMG signals as well as the contribution of muscle fiber composition in relation to responding to unexpected walking perturbations in other populations (e.g., older adults, CVA, Parkinson's disease).

In summary, we were able to provide evidence for changes in total spectral power in lower limb muscles and different muscle activation patterns in response to unannounced perturbations during walking. Results suggest different force generation mechanisms for the TA and VL. This is likely due to the muscle architecture and functional demands. In addition, it supports the notion that muscle fibers type IIa and IIb are required for rapid and effective balance recovery. As well as the notion that balance recovery processes extend past the first 2-3 steps. In terms of clinical rehabilitation, speed development and plyometric training is required for effective balance recovery.

Acknowledgements

This study was supported in part by funding from the Israeli Ministry of Science and Technology, grant #3-12072, and from the Israel Science Fund, grant #3-14527. The research is part of one contributor's (UR) work towards a doctoral degree from Ben-Gurion University of the Negev and was partially supported by a stipend.

References

1. **Asmussen MJ**, **von Tscharner V**, **Nigg BM**. Motor unit action potential clustering—theoretical consideration for muscle activation during a motor task. *Frontiers in Human Neuroscience* 12, 2018. doi: 10.3389/fnhum.2018.00015.

2. **Berger W**, **Dietz V**, **Quintern J**. Corrective reactions to stumbling in man: neuronal co-ordination of bilateral leg muscle activity during gait. *The Journal of Physiology* 357: 109–125, 1984. doi: 10.1113/jphysiol.1984.sp015492.

3. **Brauer SG**, **Woollacott M**, **Shumway-Cook A**. The influence of a concurrent cognitive task on the compensatory stepping response to a perturbation in balance-impaired

and healthy elders. *Gait and Posture* 15: 83–93, 2002. doi: 10.1016/S0966-6362(01)00163-1.

4. **Bruijn SM**, **van Dieën JH**. Control of human gait stability through foot placement. *Journal of the Royal Society Interface* 15 Royal Society Publishing: 2018.

5. **Chan CK**, **Timothy GF**, **Yeow CH**. Comparison of mean frequency and median frequency in evaluating muscle fiber type selection in varying gait speed across healthy young adult individuals. In: *Proceedings of the Annual International Conference of the IEEE Engineering in Medicine and Biology Society, EMBS*. Institute of Electrical and Electronics Engineers Inc., 2016, p. 1725–1728.

6. **Chvatal SA**, **Ting LH**. Common muscle synergies for balance and walking. *Frontiers in Computational Neuroscience*, 2013. doi: 10.3389/fncom.2013.00048.

7. **de Luca CJ**. The use of surface electromyography in biomechanics. In: *Journal of Applied Biomechanics*. Human Kinetics Publishers Inc., p. 135–163.

8. **de Luca CJ**, **Gilmore LD**, **Kuznetsov M**, **Roy SH**. Filtering the surface EMG signal: Movement artifact and baseline noise contamination. *Journal of Biomechanics* 43: 1573–1579, [date unknown]. doi: 10.1016/j.jbiomech.2010.01.027.

9. **Desmedt JE**, **Godaux E**. Ballistic contractions in man: characteristic recruitment pattern of single motor units of the tibialis anterior muscle. *The Journal of Physiology* 264: 673–693, 1977. doi: 10.1113/jphysiol.1977.sp011689.

10. **Dimitrova NA**, **Dimitrov G v.** Interpretation of EMG changes with fatigue: Facts, pitfalls, and fallacies. *Journal of Electromyography and Kinesiology* 13: 13–36, 2003. doi: 10.1016/S1050-6411(02)00083-4.

11. **Fling BW**, **Knight CA**, **Kamen G**. Relationships between motor unit size and recruitment threshold in older adults: Implications for size principle. *Experimental Brain Research* 197: 125–133, 2009. doi: 10.1007/s00221-009-1898-y.

12. **Garcia-Retortillo S**, **Rizzo R**, **Wang JWJL**, **Sitges C**, **Ivanov PC**. Universal spectral profile and dynamic evolution of muscle activation: A hallmark of muscle type and physiological state. *Journal of Applied Physiology* 129: 419–441, 2020. doi: 10.1152/japplphysiol.00385.2020.

13. **Gregory CM**, **Vandenborne K**, **Dudley GA**. Metabolic enzymes and phenotypic expression among human locomotor muscles. *Muscle and Nerve* 24: 387–393, 2001. doi: 10.1002/1097-4598(200103)24:3<387::AID-MUS1010>3.0.CO;2-M.

14. **Gronwall D**, **Wrightson P**. Delayed recovery of intellectual function after minor head injury. *The Lancet* 304: 605–609, 1974. doi: 10.1016/S0140-6736(74)91939-4.

15. **Henneman E**, **Somjen G**, **Carpenter DO**. Functional significance of cell size in spinal motoneurons. *Journal of neurophysiology* 28: 560–580, 1965. doi: 10.1152/jn.1965.28.3.560.

16. **Hermens HJ**, **Freriks B**, **Disselhorst-Klug C**, **Rau G**. Development of recommendations for SEMG sensors and sensor placement procedures. *Journal of Electromyography and Kinesiology* 10: 361–374, 2000. doi: 10.1016/S1050-6411(00)00027-4.

17. **Hof AL**. The "extrapolated center of mass" concept suggests a simple control of balance in walking. *Human Movement Science* 27: 112–125, 2008. doi: 10.1016/j.humov.2007.08.003.

18. **Hof AL**, **Duysens J**. Responses of human hip abductor muscles to lateral balance perturbations during walking. *Experimental Brain Research* 230: 301–310, 2013. doi: 10.1007/s00221-013-3655-5.

19. **Hof AL**, **Duysens J**. Responses of human ankle muscles to mediolateral balance perturbations during walking. *Human Movement Science* 57: 69–82, 2018. doi: 10.1016/j.humov.2017.11.009.

20. **Hof AL**, **Vermerris SM**, **Gjaltema WA**. Balance responses to lateral perturbations in human treadmill walking. *Journal of Experimental Biology* 213: 2655–2664, 2010. doi: 10.1242/jeb.042572.

21. **Horak FB**. Postural orientation and equilibrium: What do we need to know about neural control of balance to prevent falls? In: *Age and Ageing*. 2006.

22. **Huigen E**, **Peper A**, **Grimbergen CA**. Investigation into the origin of the noise of surface electrodes. *Medical and Biological Engineering and Computing* 40: 332–338, 2002. doi: 10.1007/BF02344216.

23. **Hussain MS**, **Mamun M**. Effectiveness of the wavelet transform on the surface EMG to understand the muscle fatigue during walk. *Measurement Science Review* 12 Sciendo: 28–33, 2012.

24. **Jacobs J v.**, **Horak FB**. Cortical control of postural responses. In: *Journal of Neural Transmission*. Springer, p. 1339–1348.

25. **Kopelman PG**. Obesity as a medical problem. *Nature* 404 Macmillan Magazines Ltd: 635–643, 2000.

26. **Kukulka CG**, **Clamann HP**. Comparison of the recruitment and discharge properties of motor units in human brachial biceps and adductor pollicis during isometric contractions. *Brain Research* 219: 45–55, 1981. doi: 10.1016/0006-8993(81)90266-3.

27. **Kupa EJ**, **Roy SH**, **Kandarian SC**, **De CJ**. *Effects of muscle fiber type and size on EMG median frequency and conduction velocity*. 1995.

28. **Lajoie Y**, **Teasdale N**, **Bard C**, **Fleury M**. Attentional demands for static and dynamic equilibrium. *Experimental Brain Research* 97: 139–144, 1993. doi: 10.1007/BF00228824.

29. **Lee BC**, **Martin BJ**, **Thrasher TA**, **Layne CS**. The effect of vibrotactile cuing on recovery strategies from a treadmill-induced trip. *IEEE Transactions on Neural Systems and Rehabilitation Engineering* 25: 235–243, 2017. doi: 10.1109/TNSRE.2016.2556690.

30. **Little CE**, **Woollacott M**. EEG measures reveal dual-task interference in postural performance in young adults. *Exp Brain Res* 233: 27–37, 2015. doi: 10.1007/s00221-014-4111-x.

31. **Mochizuki G**, **Boe SG**, **Marlin A**, **McIlroy WE**. Performance of a concurrent cognitive task modifies pre- and post-perturbation-evoked cortical activity. *Neuroscience* 348: 143–152, 2017. doi: 10.1016/j.neuroscience.2017.02.014.

32. **Mueller J**, **Martinez-Valdes E**, **Stoll J**, **Mueller S**, **Engel T**, **Mayer F**. Differences in neuromuscular activity of ankle stabilizing muscles during postural disturbances: A gender-specific analysis. *Gait and Posture* 61: 226–231, 2018. doi: 10.1016/j.gaitpost.2018.01.023.

33. **Norrie RG**, **Maki BE**, **Staines · W Richard**, **Mcilroy WE**. The time course of attention shifts following perturbation of upright stance. *Exp Brain Res* 146: 315–321, 2002. doi: 10.1007/s00221-002-1172-z.

34. **Olson CB**, **Carpenter DO**, **Henneman E**. Orderly Recruitment of Muscle Action Potentials: Motor Unit Threshold and EMG Amplitude. *Archives of Neurology* 19: 591–597, 1968. doi: 10.1001/archneur.1968.00480060061008.

35. **Papagiannis GI**, **Triantafyllou AI**, **Roumpelakis IM**, **Zampeli F**, **Garyfallia Eleni P**, **Koulouvaris P**, **Papadopoulos EC**, **Papagelopoulos PJ**, **Babis GC**. Methodology of surface electromyography in gait analysis: review of the literature. *Journal of Medical Engineering & Technology* 43: 59–65, 2019. doi: 10.1080/03091902.2019.1609610.

36. **Patel PJ**, **Bhatt T**. Attentional demands of perturbation evoked compensatory stepping responses: Examining cognitive-motor interference to large magnitude forward perturbations. *Journal of Motor Behavior* 47: 201–210, 2015. doi: 10.1080/00222895.2014.971700.

37. **Plotnik M**, **Azrad T**, **Bondi M**, **Bahat Y**, **Gimmon Y**, **Zeilig G**, **Inzelberg R**, **Siev-Ner I**. Self-selected gait speed - Over ground versus self-paced treadmill walking, a solution for a paradox. *Journal of NeuroEngineering and Rehabilitation* 12: 20, 2015. doi: 10.1186/s12984-015-0002-z.

38. **Roeder L**, **Boonstra TW**, **Kerr GK**. Corticomuscular control of walking in older people and people with Parkinson's disease. *Scientific Reports* 10, 2020. doi: 10.1038/s41598-020-59810-w.

39. **Rosenblum U**, **Kribus-Shmiel L**, **Zeilig G**, **Bahat Y**, **Kimel-Naor S**, **Melzer I**, **Plotnik M**. Novel methodology for assessing total recovery time in response to unexpected perturbations while walking. *PLoS ONE* 15, 2020. doi: 10.1371/journal.pone.0233510.

40. **Seki K**, **Narusawa M**. Firing rate modulation of human motor units in different muscles during isometric contraction with various forces. *Brain Research* 719: 1–7, 1996. doi: 10.1016/0006-8993(95)01432-2.

41. **Tang PF**, **Woollacott MH**, **Chong RKY**. Control of reactive balance adjustments in perturbed human walking: Roles of proximal and distal postural muscle activity. *Experimental Brain Research* 119: 141–152, 1998. doi: 10.1007/s002210050327.

42. **Wakeling JM**, **Pascual SA**, **Nigg BM**, **von Tscharner V**. Surface EMG shows distinct populations of muscle activity when measured during sustained sub-maximal exercise. *European Journal of Applied Physiology* 86: 40–47, 2001. doi: 10.1007/s004210100508.

43. **Woollacott M**, **Shumway-Cook A**. Attention and the control of posture and gait: A review of an emerging area of research. *Gait and Posture* 16: 1–14, 2002.

44. **Yao W**, **Fuglevand AJ**, **Enoka RM**. Motor-unit synchronization increases EMG amplitude and decreases force steadiness of simulated contractions. *Journal of Neurophysiology* 83: 441–452, 2000. doi: 10.1152/jn.2000.83.1.441.

45. **Zadravec M**, **Olenšek A**, **Matjačić Z**. The comparison of stepping responses following perturbations applied to pelvis during overground and treadmill walking. *Technology and Health Care* 25: 781–790, 2017. doi: 10.3233/THC-160798.

46. **Zajac FE**, **Faden JS**. Relationship among recruitment order, axonal conduction velocity, and muscle-unit properties of type-identified motor units in cat plantaris muscle. *Journal of Neurophysiology* 53: 1303–1322, 1985. doi: 10.1152/jn.1985.53.5.1303.

47. **Zhang Y**, **Li P**, **Zhu X**, **Su SW**, **Guo Q**, **Xu P**, **Yao D**. Extracting time-frequency feature of single-channel vastus medialis EMG signals for knee exercise pattern recognition. *PLOS ONE* 12: e0180526, 2017. doi: 10.1371/journal.pone.0180526.